# Interference Estimate from the Deep Space Network High-Power Transmitter at Goldstone with Nearby Third-Generation Mobile Users at 2 Gigahertz

C. Ho[1]

*The International Telecommunications Union (ITU) has allocated 2110 to 2200 MHz for the third-generation (3G) mobile services. Part of the spectrum (2110 to 2120 MHz) was allocated for space research service and has been used by the Deep Space Network (DSN) for years for sending command uplinks to deep-space missions. Due to the extremely high power transmitted, the potential for interference to 3G users in areas surrounding the DSN Goldstone facility exists. To address this issue, a preliminary analytical study has been performed, and computer models have been developed. The goal is to provide a theoretical foundation and tools to estimate the strength of the interference as a function of distance from the transmitter for various interference mechanisms (or propagation modes), and then to determine the size of the area in which 3G users are susceptible to interference from the 400-kW transmitter at Goldstone. The focus is non-line-of-sight interference, taking into account terrain shielding, anomalous propagation mechanisms, and technical and operational characteristics of the DSN and the 3G services.*

## I. Introduction

The International Mobile Telecommunications (IMT-2000), also known as third-generation (3G) wireless, has been allocated 2110 to 2200 MHz for its mobile services [1–5]. Part of the frequency band has been used for space research services for many years. NASA is using the 2110- to 2120-MHz band for high-power uplink transmissions at its Deep Space Network (DSN) facility at Goldstone, California. Thus, the 3G mobile receivers likely will experience interference in the 2110- to 2120-MHz frequency band when operating in the areas surrounding Goldstone. This study is going to develop a tool to model and simulate these interference effects.

The severity and duration of such interference would depend on many factors: the frequency channel assigned to the mobile unit, the time of day, the power of transmission at Goldstone, and the orientation of the transmitting antenna. The interference intensity strongly depends on the terrain profile between

[1] Communications Architectures and Research Section.

The research described in this publication was carried out by the Jet Propulsion Laboratory, California Institute of Technology, under a contract with the National Aeronautics and Space Administration.

Goldstone and the mobile unit and on weather conditions in the area. At very small percentages of time, the interference can propagate trans-horizontally through anomalous modes with little attenuation [6]. In order to assess the geographic extent of this potential interference, an interference contour map needs to be developed based on (1) characteristics of anticipated 3G mobile receivers, (2) the DSN antennas and high-power transmitter, and (3) microwave propagation models, which include terrain diffraction, atmospheric scattering, ducting and rain scattering, etc.

In this study, we use the International Telecommunications Union (ITU) propagation models to estimate the distance of potential interference that may be received by 3G users around the Goldstone 70-m transmitter antenna by taking into account terrain effects [6–10]. These distances are those at which the radiation levels from DSN transmissions exceed the IMT-2000 permissible interference levels for a given percentage of time [6]. Computer software is developed to calculate the interference level from all types of propagation modes, including line of sight and non-line of sight [5]. Firstly, we perform the terrain profile analysis to identify whether the path between transmitter and receiver is line of sight or trans-horizon. The terrain diffraction loss is calculated through multi-mountain tops for each terrain profile. Then attenuations through two anomalous propagation modes (modes 1 and 2) after a terrain-shielding correction are studied at a small percent of time. Finally, propagation losses through all modes are compared, and the minimum loss at each direction is determined. Based on the loss, contours are drawn around the DSN Goldstone station for 3G mobile users.

## II. Propagation by Terrain Diffraction

### A. Terrain Around Goldstone Site

The DSN's Deep Space Station 14 (DSS 14) is a 70-m antenna located in the Mojave Desert, an area filled with bare hills and dry lakes. With an elevation of 1,002 m above sea level, the antenna is surrounded by hills on the southeast, west, and north sides. The hill elevations range from 1400 m to 1700 m. Figure 1 is a photo showing the 70-m antenna, while Fig. 2 is an elevation map showing the surrounding terrain environment. These terrains normally would prevent line-of-sight interference and would offer significant interference protection for the DSN and other users of the spectrum sharing the same frequency bands.

Two open valleys lie toward the east and northwest sides of the antenna. However, immediately to the south side of the antenna, there are two small hills with an elevation of about 1100 m, blocking the view of the antenna with an elevation angle of $\sim$2 deg. The surrounding terrain elevation angles have important effects on interference propagation through diffraction and ducting, as we show later. Hills with larger elevation angles block the interference signals by increasing the attenuation of the propagation. Figure 3 shows the surrounding terrain elevation angles relative to the mechanical center of the 70-m antenna, which is about 37 m above the ground. A large mountain lies at the north side of the antenna, with a maximum elevation angle of 4.8 deg. At the east and northwest sides, terrain elevation angles relative to the antenna are lower (1.0 to 1.2 deg) due to open valleys. The antenna is mechanically unable to point below 6 deg. The antenna does not transmit signals when its elevation angle is less than 10 deg.

### B. Diffraction Losses over the Terrain

The S-band (around 2-GHz) interference signals can propagate beyond the line of sight through hilltop diffraction [10]. For the terrain diffraction calculation, we used the Goldstone–Los Angeles path as an example because a metropolitan area with a large community of 3G users is our major concern. The terrain profile from the Goldstone 70-m transmitter (point T) to downtown Los Angeles (point L) along a 215-deg azimuth cut is shown in Fig. 4. The terrain elevation has been modified and plotted on a curved spherical Earth surface with a 4/3 Earth radius. We can from the left side of Fig. 4 that there are several small hills in the Mojave desert highland. The high terrain of the San Gabriel Mountains on the Los

**Fig. 1. The 70-m antenna (DSS 14) at Goldstone, California, against the background of the Mojave Desert. The valley behind the antenna is approximately in the eastern direction. Another station's (DSS 15's) 34-m antenna in the southeast side can also be seen in the background.**

Angeles side shields a large amount of any interference signals. We used a standard method [10], which the ITU recommended, to calculate the diffraction losses from the transmitter T to points A, C, E, G, and L as marked in the plot.

The diffraction losses through the hilltops depend on the angular distance (steepness) of the hill and the distance. The angular distance, $\theta$, is the angle in radians between two horizon rays across the hilltops concerned in the great circle plane:

$$\theta = \frac{d}{a_e} + \theta_{et} + \theta_{er} \tag{1}$$

where $d$ is the distance between the transmitter and receiver at sea level and $a_e$ is the median effective Earth radius (where $a_e = 8930$ km because of the average annual refractivity gradient, $\Delta N = 45$, at Goldstone). The horizon ray elevation angles (in radians) $\theta_{et}$, relative to the transmitter, and $\theta_{er}$, relative to the receiver, may be computed using the following equations:

$$\theta_{et} = \frac{h_{Lt} - h_{ts}}{d_{Lt}} - \frac{d_{Lt}}{2a_e} \tag{2}$$

and

$$\theta_{er} = \frac{h_{Lr} - h_{rs}}{d_{Lr}} - \frac{d_{Lr}}{2a_e} \tag{3}$$

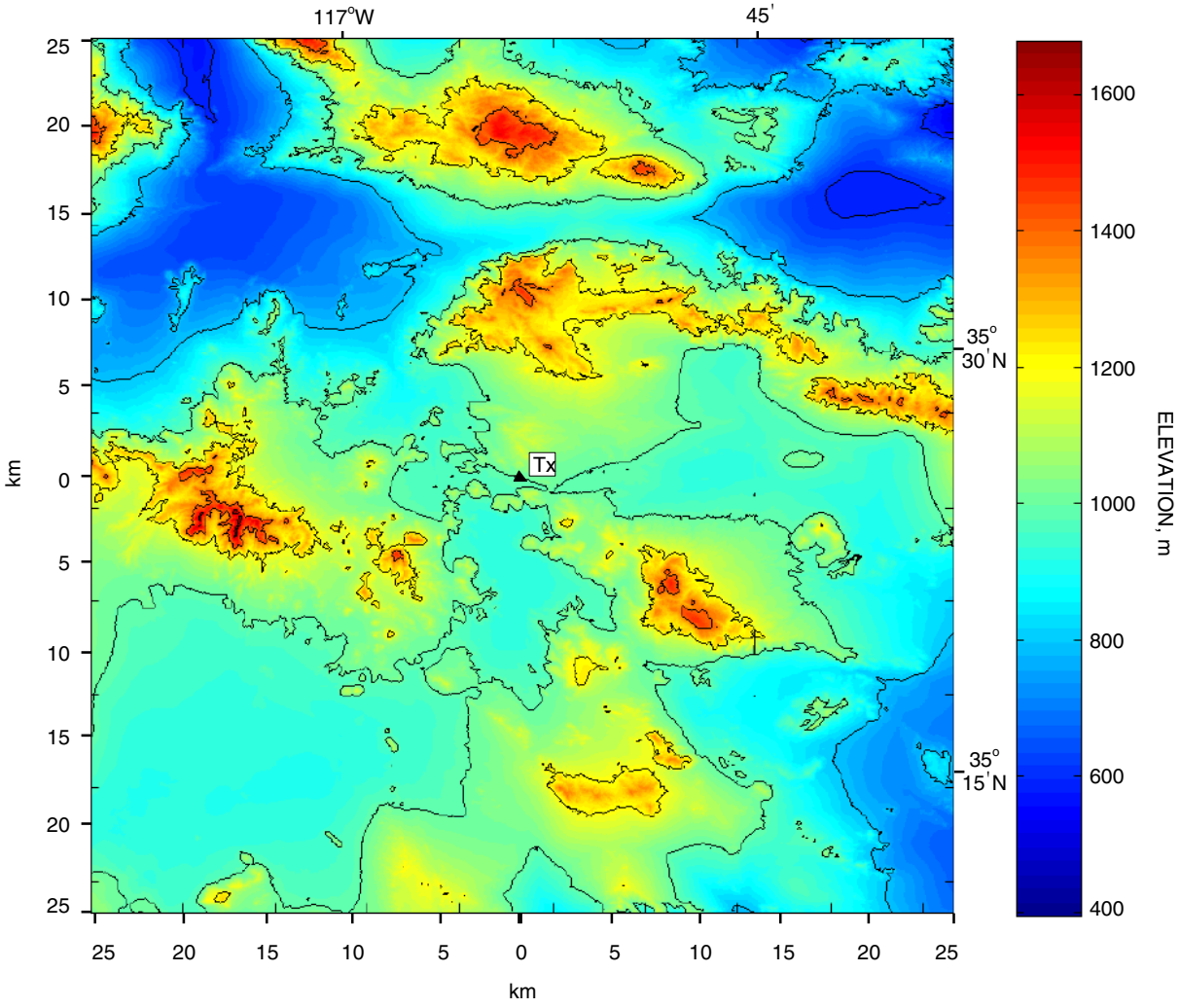


**Fig. 2. The terrain elevation around the Goldstone 70-m transmitter. The map is centered at the antenna (triangle mark) with each side extended 25 km. There are some small hills to the south side of the transmitter. There are some open areas nearby on the east and west sides, and a large mountain lies on the north side.**

where $h_{Lt}$ and $h_{Lr}$ are the elevations of horizon obstacles and $h_{ts}$ and $h_{rs}$ are the elevations of transmitting and receiving antennas, respectively, all above the average mean sea level (AMSL). The $d_{Lt}$ and $d_{Lr}$ are sea-level arc distances from each antenna to its radio horizon obstacle.

The diffraction loss for a simplified single knife-edge is

$$J(\nu) = 6.9 + 20\log\left(\sqrt{(\nu-0.1)^2+1}+\nu-0.1\right) \quad \text{dB} \tag{4}$$

where the parameter $\nu$ is defined as

$$\nu = \theta\sqrt{\frac{2d_{lt}d_{lr}}{\lambda d}} \tag{5}$$

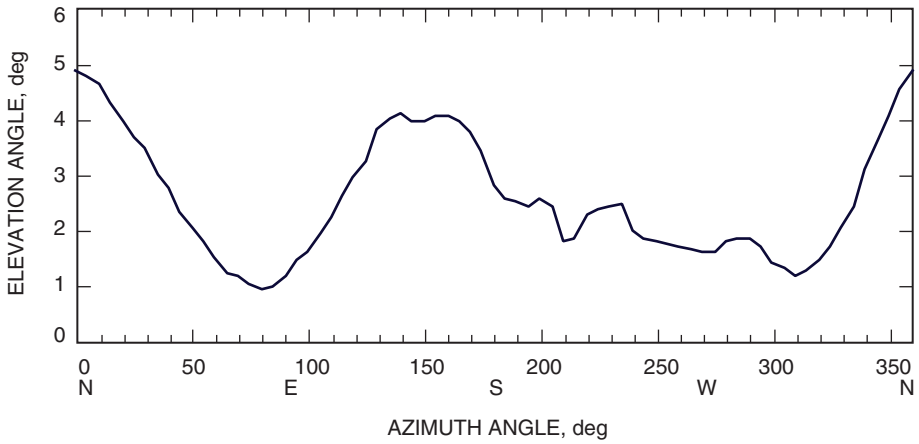


**Fig. 3. Terrain elevation angles relative to the center of the 70-m antenna at Goldstone.**

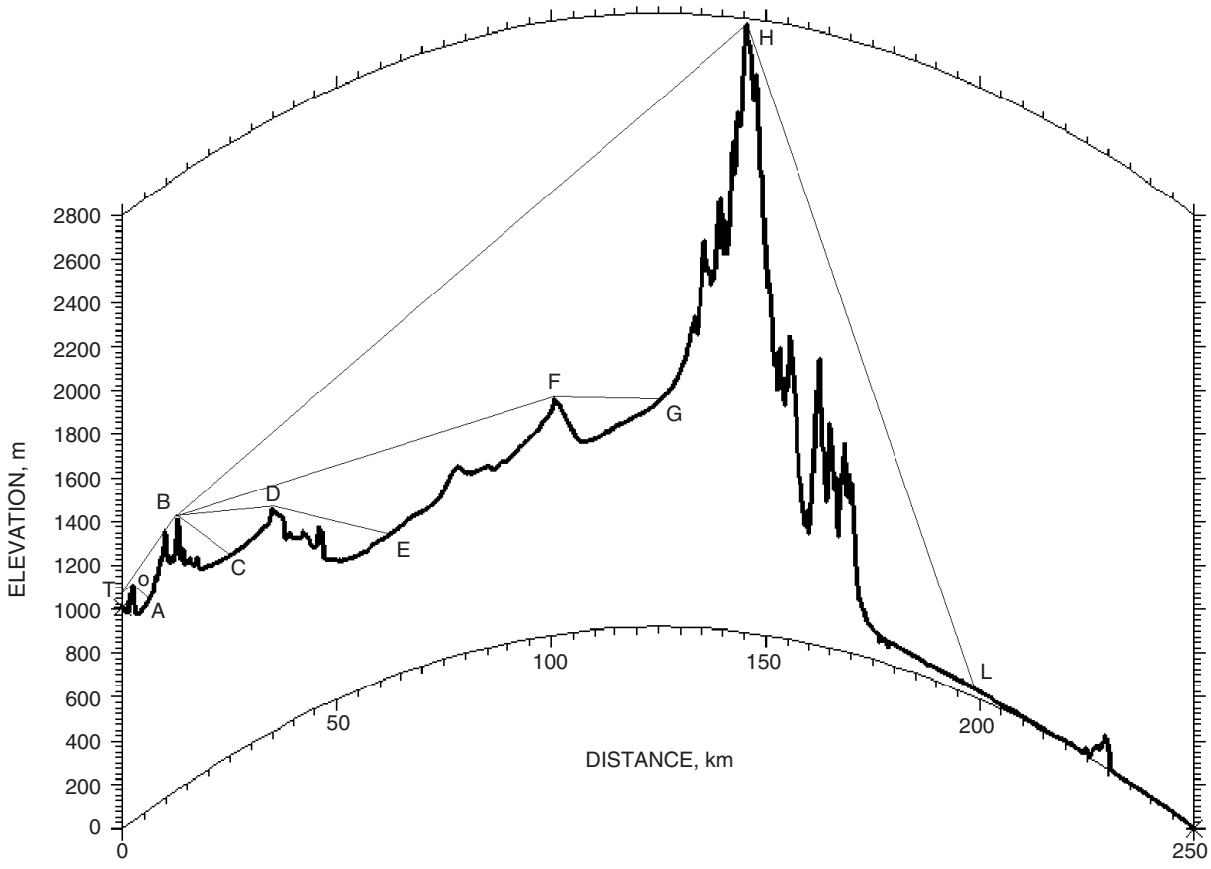


**Fig. 4. The terrain profile from the Goldstone 70-m antenna (left) to Los Angeles (right). This is a cut along the 215-deg azimuth angle relative to the transmitter site (0 deg points to the north).**

where angular distance, $\theta$, is from Eq. (1) and wavelength, $\lambda$, is $1.42 \times 10^{-4}$ km for the radio wave at S-band (2.11 GHz).

In a double knife-edge situation based on the method recommended in ITU-R P.526 [10], the diffraction loss over the two hilltops is simplified as the sum of diffraction losses over each knife-edge.

Finally, the total diffraction losses through the terrain are

$$L_d = L_{fs} + L_{df} \tag{6}$$

where $L_{fs}$ is free-space transmission loss through a distance $d$:

$$L_{fs} = 32.45 + 20 \log f + 20 \log d \tag{7}$$

Table 1 lists all parameters and preliminary estimates of total diffraction losses from transmitter T over several hilltops to points A, C, E, G, and L, respectively (as shown in Fig. 4), along the Goldstone–Los Angeles terrain profile. Actual losses should be larger than those shown in Table 1 because most hills have rounded tops and rough surfaces, instead of sharp knife-edges. The rounded hilltops have additional curvature loss of 10 to 20 dB.

The DSN 70-m antenna boresight gain is 62 dB, and back-lobe gain (<48 deg) is −10 dB. Because the antenna always transmits the beam above the 30-deg elevation angle, its corresponding side-lobe gain is less than −7 dB. Using the relation $P_r = P_t + G_t + G_r - L_d$, we can calculate the interference power received at the different distances. From Table 1, we can see that when the transmitter power is 20 kW and the 3G receiver antenna gain, $G_r$, is 0 dB, the interference power received by an IMT-2000 user is less than −109 dBm (the threshold we used), within a range of about 35 km from the transmitter site. This is shown in the last column of Table 1. When output power is 400 kW (a 13-dB increase), the range will be limited to 50 km. In the Los Angeles area, the interference power is far below the threshold because the San Gabriel Mountains alone can cause the 76.9-dB diffraction attenuation (not including free-space loss). Thus, interference through terrain diffraction can play a role only within a 50-km range from the transmitter, depending largely on the mountain topography.

Figure 5 shows the contours for terrain diffraction effects alone with two types of transmitting powers (20 kW and 400 kW). Beyond the contour lines, interference through the terrain diffraction received

**Table 1. Diffraction losses over hilltops along the Goldstone–Los Angeles terrain profile.**

| Path | $d$, km | $h_{lt}$, m | $h_{ts}$, m | $d_{lt}$, km | $h_{rs}$, m | $d_{lt}$, km | $\theta_{et}$, $10^{-3}$ | $\theta_{er}$, $10^{-3}$ | $\theta$, $10^{-3}$ | $\nu$ | $J(\nu)$, dB | $L_{df}$, dB | $L_{fs}$, dB | $L_d$, dB | $P_r$, dBm |
|---|---|---|---|---|---|---|---|---|---|---|---|---|---|---|---|
| TOA | 15 | 1075 | 1002 | 6 | 930 | 9 | 11.84 | 15.61 | 29.13 | 6.56 | 29.2 | 29.2 | 113 | 142.2 | −72.2 |
| TBC | 25 | 1250 | 1002 | 13.5 | 910 | 11.5 | 17.61 | 28.92 | 49.33 | 14.5 | 36.2 | 36.2 | 127 | 163.2 | −97.2 |
| TBD | 35 | 1250 | 1002 | 13.5 | 950 | 21.5 | 17.61 | 13.17 | 34.7 | 11.86 | 34.4 | at $E$ | | | |
| BDE | 49 | 950 | 1250 | 22 | 675 | 27 | −14.9 | 8.68 | −0.71 | −0.29 | 3.6 | 38.0 | 155 | 193.0 | −126.8 |
| TBF | 101 | 1250 | 1002 | 13.5 | 1095 | 87.5 | 17.61 | −3.13 | 25.79 | 10.47 | 33.3 | at $G$ | | | |
| BFG | 111.5 | 1095 | 1250 | 87.5 | 1025 | 24 | −6.67 | 1.58 | 7.4 | 3.8 | 24.4 | 57.7 | 162 | 219.7 | −153.7 |
| TBH | 145 | 1250 | 1002 | 13.5 | 2800 | 131.5 | 17.61 | −19.15 | 14.66 | 6.09 | 29.5 | at $L$ | | | |
| BHL | 186.5 | 2800 | 1250 | 131.5 | 75 | 55 | 4.43 | 46.47 | 71.78 | 53.05 | 47.4 | 76.9 | 166 | 242.9 | −177.3 |

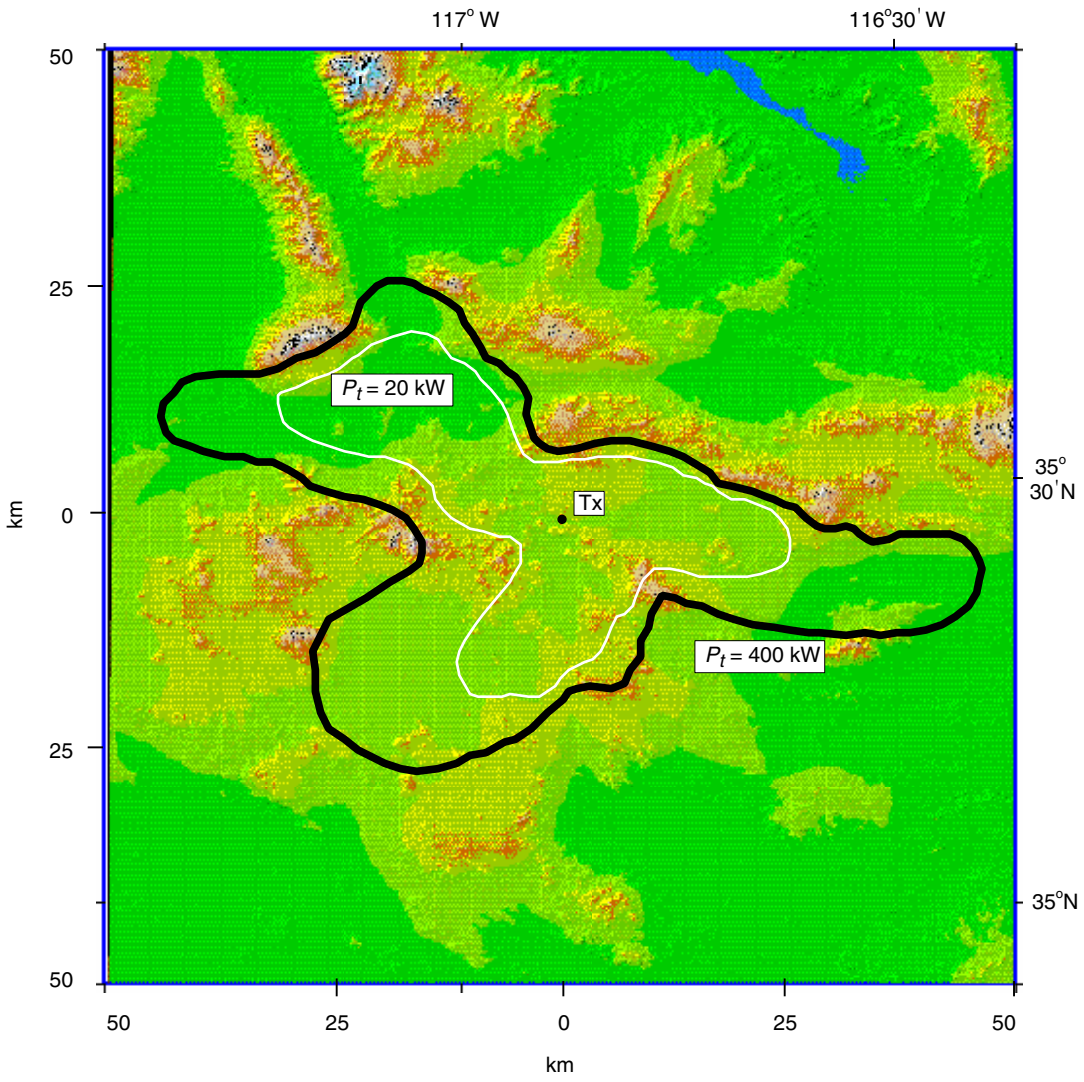


**Fig. 5. The distance of potential interference around the Goldstone 70-m antenna for terrain diffraction alone. The interference signals will attenuate to below the IMT-2000 user's threshold (–109 dBm) outside the white line (for 20-kW transmitting power) and the black line (for 400-kW power).**

by 3G mobile systems will be below the threshold. Because the interference signals are greatly blocked by the mountains (e.g., at the northeast side), the contour lines are aligned with the major mountain's orientation near the transmitter. However, in some directions without major mountains, contours can extend further, where the interference signals attenuate mainly through the spherical Earth curvature losses. Because the diffraction loss is almost independent of changes in time percent, the results shown in Fig. 5 can be applied to a large percent of time.

## III. Interference Through Anomalous Modes

Although interference through terrain diffraction is quickly attenuated within a 50-km range, it may suffer only little attenuation and can propagate to a large distance through two anomalous modes, as shown in Fig. 6 [6–8,11]: at a very small percentage of time, mode 1 (which is due to atmospheric effects during clear weather and propagates along the great circle, such as tropospheric scattering and

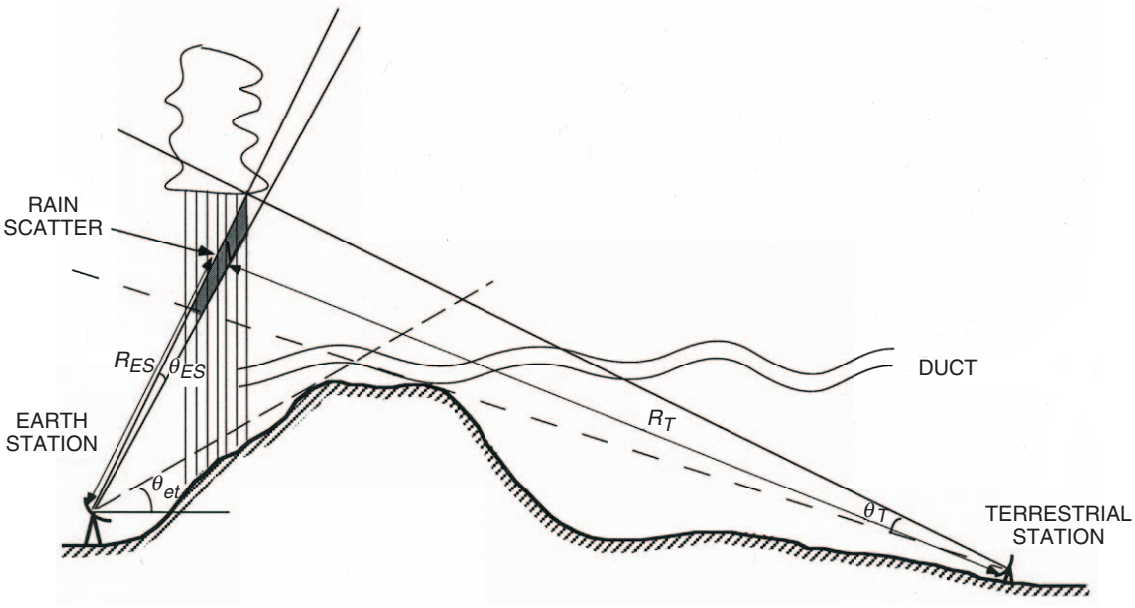


**Fig. 6. Two interference mechanisms between a DSN transmitter (Earth station) and IMT-2000/UMTS customers (terrestrial station) beyond the line of sight. Rain scattering by a common viewed rain region and ducting propagation through a surface or elevated duct can cause interference problems a very small percentage of time.**

atmospheric ducting) and mode 2 (which can be off the great circle, such as rain scattering or other hydrometeor scattering). As a result, the interference power may greatly exceed the threshold of 3G mobile phone at a small percentage of time at a distance that is defined in the previous section by terrain diffraction. Also, we need to take into account terrain-shielding effects on both anomalous modes.

### A. Attenuation Through Mode 1 [7,8,11]

As shown in Fig. 6, when the atmosphere has strong vertical gradients, propagating waves pointing slightly upward can be trapped within the duct between the ground and a reflected atmospheric layer or within an elevated ducting layer and propagate for a long distance. Tropospheric turbulences and irregularities also can scatter the interference into a large area, which usually defines the background noise level. However, after including the terrain-shielding effects on the transmitting antenna, the interference power through these modes can be significantly reduced.

For the Goldstone site, the surrounding hilltop has a maximum elevation angle of 4.85 deg relative to the 70-m transmitting antenna at the north and a minimum angle of 1.1 deg at the east. Using the maximum correction ($A_h$ = 30 dB), which corresponds to the elevation angle of the transmitter (see Fig. 3), $\theta_{et} \geq 3$ deg, the received interference powers for various time percentages are shown in Fig. 7. The transmitter antenna side-lobe gain, $G_t = -7$ dB, and receiving antenna gain, $G_r = 0$ dB, are used for this calculation. When elevation angles are between 1 deg and 3 deg, the loss correction is less than 30 dB (e.g., $\theta_{et} = 1$ deg, $A_h = 18.8$ dB; $\theta_{et} = 2$ deg, $A_h = 25.5$ dB). The preliminary estimates of distances of potential interference for various percentages of time with maximum terrain shielding (3-deg elevation angle) and without terrain shielding (0-deg elevation) are shown in Table 2. Thus, actual distances should be in a range between the maximum and minimum distances shown in Table 2. For example, for 400-kW transmitting power, the potential interference distance is 160 km for 1-deg elevation shielding and 120 km for 2 deg at 1.0 percent of time.

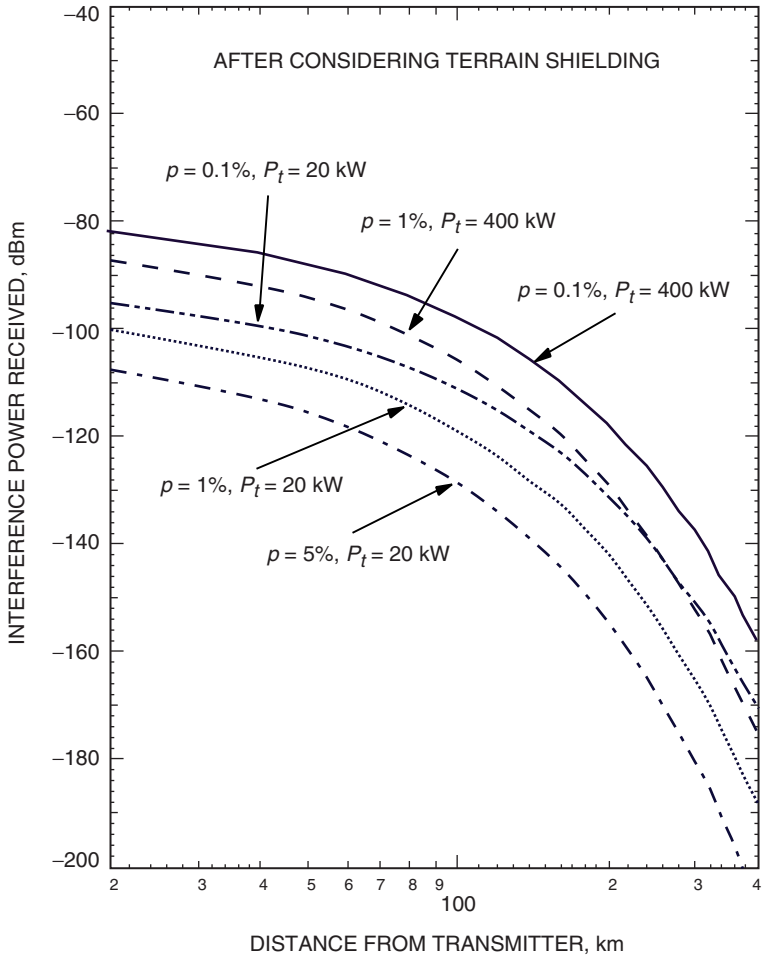


**Fig. 7. Preliminary estimate of interference power received through mode 1 with mountain shielding effects (additional 30-dB loss).**

**Table 2. Distances of potential interference through mode 1 for a –109 dBm threshold.**

| Percent of time | Without mountain shielding, km | | With mountain shielding, km | |
|---|---|---|---|---|
| | $P_t = 20$ kW | $P_t = 400$ kW | $P_t = 20$ kW | $P_t = 400$ kW |
| $p = 0.1\%$ | 235 | 305 | 90 | 160 |
| $p = 1.0\%$ | 185 | 240 | 60 | 110 |
| $p = 5.0\%$ | 138 | 190 | 24 | 72 |

### B. Attenuation Through Mode 2 [12,13]

We also need to investigate the possibility of interference signals propagating through rain scattering. Even though the rainfall rate is very low in the Goldstone desert area, rain scattering can make it possible for waves to propagate into an area beyond the line of sight. Rain droplets can reflect and scatter the waves like a mirror between a transmitter and a trans-horizon receiver. Terrain is expected to have little effect on rain-scattering propagation, except for mountain peaks with very large elevations that can block direct illumination from rain clouds.

Figure 8 shows interference powers generated through the rain-scattering mode as a function of distance for various time percentages $p$. It indicates that the effect of rain scattering would only exceed the threshold less than 1.0 percent of the time at distances within 10 km for 20-kW transmitting power and 42 km for 400-kW power. The distances of potential interference for various percentages of time are shown in Table 3, assuming a −109 dBm threshold. Compared with mode 1, rain scattering appears to be insignificant because of the much smaller distance due to a lower rainfall rate.

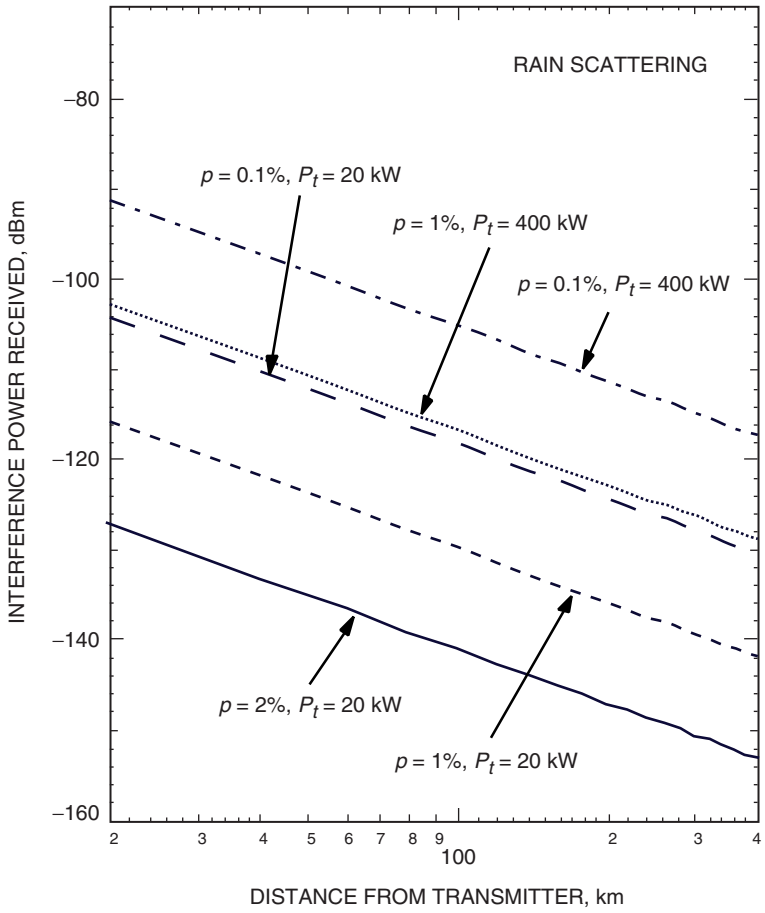


**Fig. 8. Preliminary estimate of received interference powers through rain-scattering modes as a function of distance from the DSN Goldstone transmitter for various percentages of time.**

**Table 3. Distances of potential interference through rain scattering.**

| Percent of time | $P_t = 20$ kW, km | $P_t = 400$ kW, km |
|---|---|---|
| $p = 0.1\%$ | 35 | 155 |
| $p = 1.0\%$ | ∼10 | 42 |
| $p = 2.0\%$ | <10 | ∼10 |

## IV. Potential Interference Area Through All Propagation Modes

After taking the terrain into account, we have developed a preliminary contour map that includes all propagation modes (diffraction, modes 1 and 2) as shown in Fig. 9 for two transmitting power levels under the 1 percent of time probability. We found that the terrain diffraction propagation has larger attenuation and smaller distance of potential interference than do modes 1 and 2. Depending on the surrounding terrain profiles, the interference signals due to diffraction quickly decrease to below the threshold of the 3G mobile systems within a range from 35 km to 50 km. The diffraction effect can be neglected at large distances.

We also found that rain-scattering (mode 2) propagation also has a larger loss and smaller interference distance (10 to 42 km at 1 percent of time). This is because of only a very small rain-scattering effect on S-band and low rainfall rates at Goldstone.

Because mode 1 has a smaller loss and a longer interference distance than do terrain diffraction and rain scattering, the final interference distances are basically determined by mode 1. There are some significant differences in the distances with and without terrain shielding around the transmitting antenna. The actual distance is between 110 km (3-deg elevation shielding) and 170 km (1-deg elevation shielding) from the Goldstone site for a 400-kW transmitting power at 1 percent of the time. For a 20-kW transmitting power, the distance is between 60 km and 110 km. In the north and southeast directions, because of the larger terrain elevation angles around the transmitting antenna, there are shorter distances of potential interference from the Goldstone site. In the east and northwest directions, the distances are much larger because of lower elevation angles of the surrounding terrain. In the south and southwest sides, the potential interference contour for 400-kW transmitting power extends to near the San Gabriel Mountains, which can block a great deal of mode 1 transmission from the receiving side in the Los Angeles area.

As shown in Fig. 9, both Los Angeles and Las Vegas are just outside of the potential interference contour and are free from interference at least 99 percent of the time. Therefore, we conclude that, for a very small percentage of time (1 percent), mode 1 will be a dominant interference mechanism and will have the largest distance among all propagation modes.

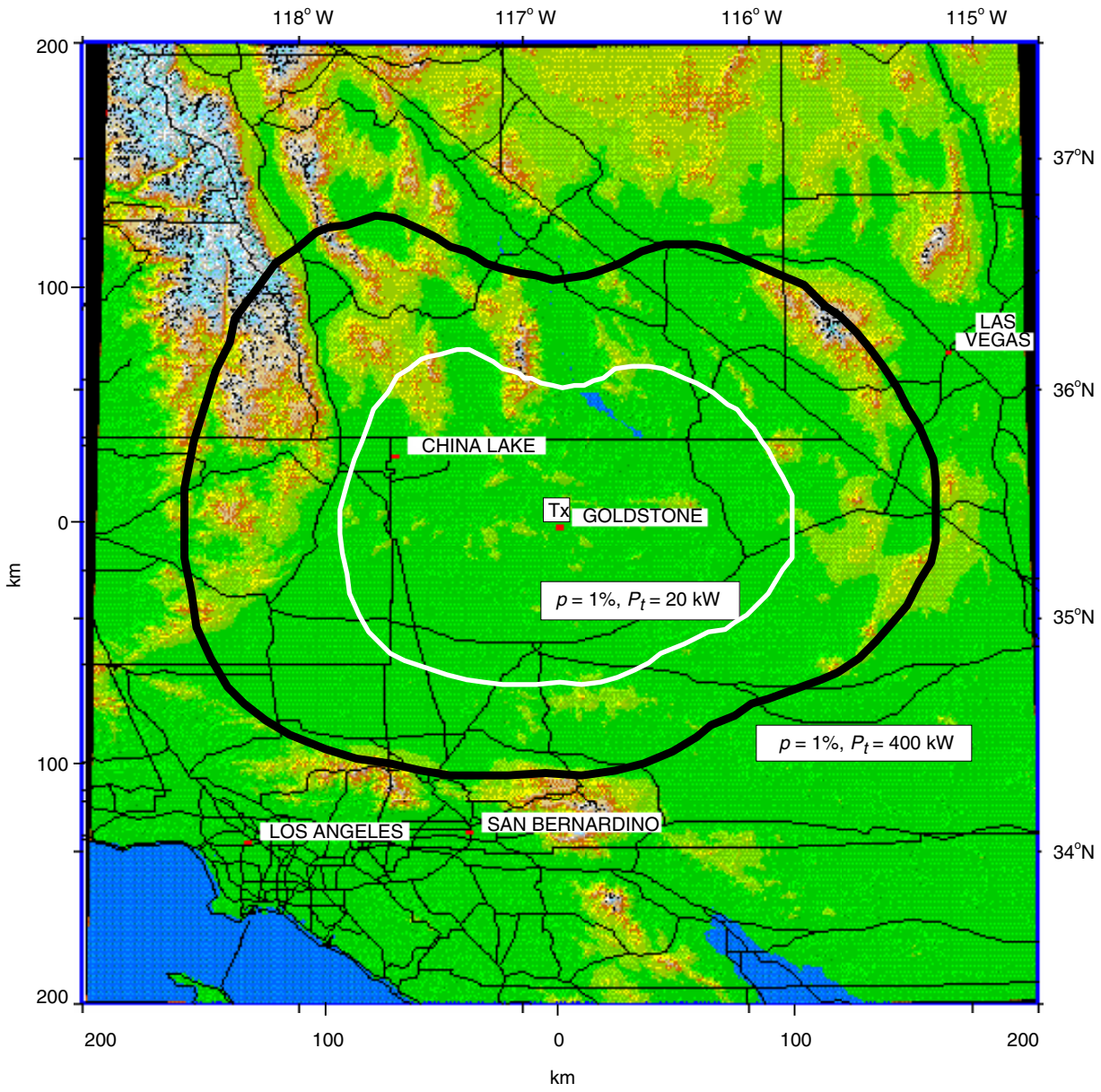


**Fig. 9. Preliminary contour map for 3G mobile users operating in areas surrounding the DSN Goldstone transmitter: transmitter power = 20 kW (white line) and 400 kW (black line); percent of time = 1. Both Los Angeles and Las Vegas are just outside of the contour and are free from interference at least 99 percent of the time.**

# References


[1] "International Mobile Telecommunications-2000 (IMT-2000)," Recommendation ITU-R M.687, 1997.

[2] "Guidelines for Evaluation of Radio Transmission Technologies for IMT-2000," Recommendation ITU-R M.1225, 1997.

[3] "Spectrum Considerations for Implementation of International Mobile Telecommunications-2000 (IMT-2000) in the Band 1885-2025 MHz and 2110-2200 MHz," Recommendation ITU-R M.1036, 1999.

[4] C. Ho, M. Sue, T. Peng, P. Kinman, and H. Tan, "Interference Effects of Deep Space Network Transmitters on IMT-2000/UMTS Receivers at S-Band," *The Telecommunications and Mission Operations Progress Report 42-142, April–June 2000*, Jet Propulsion Laboratory, Pasadena, California, pp. 1–21, August 15, 2000.
http://tmo.jpl.nasa.gov/tmo/progress_report/42-142/142A.pdf

[5] C. M. Ho, M. K. Sue, T. K. Peng, and E. K. Smith, "Terrestrial Propagation of 2-Gigahertz Emissions Transmitted from the Deep Space Network 70-Meter Antenna at Robledo," *The Interplanetary Network Progress Report 42-152, October–December 2002*, Jet Propulsion Laboratory, Pasadena, California, pp. 1–22, February 15, 2003.
http://ipnpr.jpl.nasa.gov/tmo/progress_report/42-152/152C.pdf

[6] "Prediction Procedure for the Evaluation of Microwave Interference Between Stations on the Surface of the Earth at Frequencies Above About 0.7 GHz," Recommendation ITU-R P.452-9, 1999.

[7] "Determination of the Coordination Area of an Earth Station Operating with a Geostationary Space Station and Using the Same Frequency Band as a System in a Terrestrial Service," Recommendation ITU-R IS.847-1, 1993.

[8] "Propagation Data Required for the Evaluation of Coordination Distances in the Frequency Range 100 MHz to 105 GHz," Recommendation ITU-R P.620-4, 1999.

[9] *Radio Regulations*, Edition 2001, Appendix S7 (former Appendix 28), ITU Document, Geneva, Switzerland, 2001.

[10] "Propagation by Diffraction," Recommendation ITU-R P.526-6, 1999.

[11] R. K. Crane, "A Review of Transhorizon Propagation Phenomena," *Radio Science*, vol. 16, p. 649, 1981.

[12] W. L. Flock, *Propagation Effects on Satellite Systems at Frequencies Below 10 GHz, A Handbook for Satellite Systems Design*, NASA Reference Publication 1102, 1987.

[13] CCIR, "Scattering by Precipitation," Report 882-1, in vol. V, *Propagation in Non-Ionized Media*, Recommendations and Reports of the CCIR, Geneva, Switzerland, ITU, 1986.